

## SYNTHESIS OF $\gamma$ -Fe<sub>2</sub>O<sub>3</sub> BY THERMAL DECOMPOSITION OF FERROUS GLUCONATE DIHYDRATE\*

M. M. Rahman<sup>1</sup> and A. Venkataraman<sup>2\*\*</sup>

<sup>1</sup>Nawab Shah Alam Khan Institute of Post Graduate Studies & Research Center, Anwar ul - Ullom College, Mallepally, Hyderabad – 500 001, India

<sup>2</sup>Department of Chemistry, Gulbarga University, Gulbarga – 585 106, India

(Received June 22, 2001)

### Abstract

Ferrous gluconate dihydrate (FeC<sub>12</sub>H<sub>22</sub>O<sub>14</sub>·2H<sub>2</sub>O), was prepared and its thermal decomposition was studied by means of simultaneous thermal analysis, supplemented with a two probe d.c. electrical conductivity measurements under the atmospheres of static air, dynamic air and dynamic nitrogen. Under all the atmospheres final product was found to be  $\alpha$ -Fe<sub>2</sub>O<sub>3</sub> with FeO,  $\gamma$ -Fe<sub>2</sub>O<sub>3</sub>, Fe<sub>3</sub>O<sub>4</sub> etc. as probable intermediates.  $\gamma$ -Fe<sub>2</sub>O<sub>3</sub> was formed under the atmosphere of dynamic air containing water vapour.  $\gamma$ -Fe<sub>2</sub>O<sub>3</sub> thus synthesised was characterised for its structure, morphology, thermal and magnetic behaviour.

**Keywords:** electrical conductivity,  $\gamma$ -Fe<sub>2</sub>O<sub>3</sub>, magnetic properties, structure, synthesis, thermal analysis

### Introduction

Commercially,  $\gamma$ -Fe<sub>2</sub>O<sub>3</sub> is prepared by dehydration of synthetic goethite ( $\alpha$ -FeO(OH)) to  $\alpha$ -Fe<sub>2</sub>O<sub>3</sub>, its reduction to Fe<sub>3</sub>O<sub>4</sub> and finally reoxidation to  $\gamma$ -Fe<sub>2</sub>O<sub>3</sub> [1–4].

$\gamma$ -Fe<sub>2</sub>O<sub>3</sub> particles of nanosized dimensions improves many of the required parameters for its effective use as a recording material [3–10]. The study on synthesis of  $\gamma$ -Fe<sub>2</sub>O<sub>3</sub> for recording and memory devices is continuously attaining greater significance [1, 3–5]. New synthetic routes for the synthesis of  $\gamma$ -Fe<sub>2</sub>O<sub>3</sub> are being continuously investigated, some of them include: the ion exchange reaction of NaFeO<sub>2</sub> with benzoic acid [11], thermal decomposition of lepidocrocite [12], employing sol-gel techniques [9], decompositions of microemulsions [13], and thermal decompositions of metal carboxylates under controlled conditions [14–15]. The present investigation is a continuation of our ongoing programme on study of the new routes and also em-

\* This paper is dedicated to late Prof. A. J. Mukhedkar.

\*\* Author for correspondence: E-mail: venkat1@rasms.czaronline.net.in

ploying new precursors in the synthesis of ultrafine  $\gamma$ -Fe<sub>2</sub>O<sub>3</sub> particles and having optimum properties.

In our earlier work [14–18], we have used d.c. electrical conductivity technique as a supplementary tool to thermal analysis in the study of the thermal decomposition reactions for the formation of  $\gamma$ -Fe<sub>2</sub>O<sub>3</sub>. In the present study we investigate the thermal decomposition of ferrous gluconate dihydrate (FeC<sub>12</sub>H<sub>22</sub>O<sub>14</sub>·2H<sub>2</sub>O), by conventional thermal analysis (TG/DTA/DTG) supplemented with electrical conductivity measurements, under different atmospheres.

## Experimental

### *Preparation of FeC<sub>12</sub>H<sub>22</sub>O<sub>14</sub>·2H<sub>2</sub>O*

Ferrous gluconate dihydrate was prepared by dissolving equal volumes of equimolar solutions of ferrous sulphate and barium gluconate at 60°C, in a flow of dry nitrogen under vigorous stirring. The yellowish grey precipitate of ferrous gluconate dihydrate (FeC<sub>12</sub>H<sub>22</sub>O<sub>14</sub>·2H<sub>2</sub>O), thus obtained was washed thoroughly with double distilled water and dried under vacuum. The elemental analysis of the gluconate gave, C: 28.64(29.88), H: 4.97(4.56), Fe: 12.32(11.65), the values in the parenthesis are the calculated values and satisfy the formulae FeC<sub>12</sub>H<sub>22</sub>O<sub>14</sub>·2H<sub>2</sub>O.

### *Thermal analysis*

The thermal analysis traces were obtained with Netzsch instrument under the atmosphere of static air, dynamic dry nitrogen, and dynamic dry air (100 mL min<sup>-1</sup>) from room temperature to 1000°C, with a heating rate of 10°C min<sup>-1</sup>.

### *Electrical conductivity*

The two-probe method employing a d.c. electrical conductivity method as reported earlier [16–18] was used in the present study.

### *Infrared studies*

The infrared spectra were recorded on a Perkin Elmer model 337 spectrometer using nujol mull.

### *X-ray diffraction*

The powder X-ray diffraction patterns was obtained from a PW 1730 Philips X-ray diffractometer, using CuK<sub>α</sub> radiation.

### *Magnetic hysteresis*

The magnetic hysteresis of  $\gamma$ -Fe<sub>2</sub>O<sub>3</sub> particles was investigated using a vibrating sample magnetometer-VSM (EG & G Princeton Applied Research Model 4500) magnetometer.

### Morphology

The morphology of  $\gamma$ -Fe<sub>2</sub>O<sub>3</sub> particles was investigated using Cambridge Stereo Scan 150 instrument.

## Results and discussion

### Study under static air

Figure 1 shows the thermal analysis trace of ferrous gluconate sample under static air atmosphere. In this figure the dehydration step of  $\text{FeC}_{12}\text{H}_{22}\text{O}_{14} \cdot 2\text{H}_2\text{O}$ , is indicated by a broad endothermic peak ( $\sim 108^\circ\text{C}$ ) on the DTA trace. The DTG trace also shows a broad peak (at  $108^\circ\text{C}$ ). The TG trace shows a mass loss in the temperature range  $40$ – $140^\circ\text{C}$  corresponding to the loss of two water molecules. A sample isothermally heated at  $160^\circ\text{C}$  shows that the bands due to water molecules were not present in the infrared spectrum. Elemental analysis (C, H and metal estimation) of this sample also agreed with anhydrous gluconate ( $\text{FeC}_{12}\text{H}_{22}\text{O}_{14}$ ).

The oxidative decomposition of the complex  $\text{FeC}_{12}\text{H}_{22}\text{O}_{14}$ , was indicated by the presence of four exothermic peaks on the DTA trace at  $220$ ,  $293$ ,  $350$  and  $421^\circ\text{C}$ . Broad peaks on the DTG trace at similar temperatures are noticed. However, the TG trace shows continuous mass loss from  $140$  to  $478^\circ\text{C}$ . The final mass loss corresponds to the formation of  $\alpha$ -Fe<sub>2</sub>O<sub>3</sub>. The samples isothermally heated at  $220$  and  $293^\circ\text{C}$  gave a diffuse X-ray patterns. The X-ray pattern of the sample obtained after heating at  $350^\circ\text{C}$  shows mixed phases of Fe<sub>3</sub>O<sub>4</sub> and  $\gamma$ -Fe<sub>2</sub>O<sub>3</sub>, and the sample isothermally heated at  $421^\circ\text{C}$  shows to be purely  $\alpha$ -Fe<sub>2</sub>O<sub>3</sub>. Hence it may be understood that the peaks observed on the DTA and DTG traces at  $350$  and  $421^\circ\text{C}$  are due to the transformation to more crystalline forms.

Direct current electrical (d.c.) conductivity of this compound ( $\text{FeC}_{12}\text{H}_{22}\text{O}_{14} \cdot 2\text{H}_2\text{O}$ ) under this atmosphere could not be studied since the pellet of this sample melted above  $200^\circ\text{C}$ .

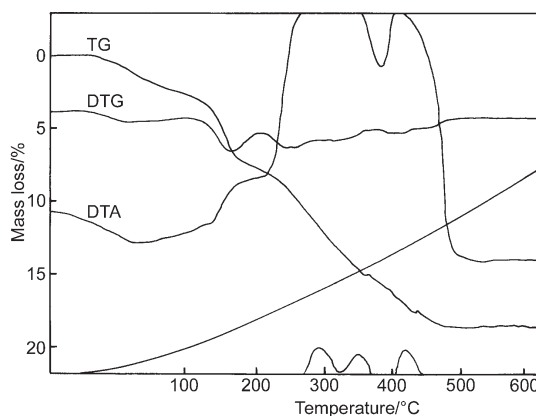


**Fig. 1** Thermal trace of  $\text{FeC}_{12}\text{H}_{22}\text{O}_{14} \cdot 2\text{H}_2\text{O}$  under static air atmosphere

When the reaction has been carried out in static air atmosphere, the gaseous product act as a gas buffer for the solid state reaction and some of the reactions will be ill-defined [17]. A study of reaction under dynamic atmospheres viz., dynamic nitrogen and dynamic air has been carried out to compare the data and clarify the results obtained therein.

#### *Study under dynamic nitrogen atmosphere*

The thermal analysis traces are shown in Fig. 2. The TG trace shows a mass loss in the temperature range ambient to 160°C, corresponding to loss of two water molecules indicating a dehydration process. The DTA trace shows an endothermic peak at 95 followed by a shoulder at 155°C. The DTG trace shows two peaks at 80 and 185°C, both these traces show the dehydration process for gluconate sample.

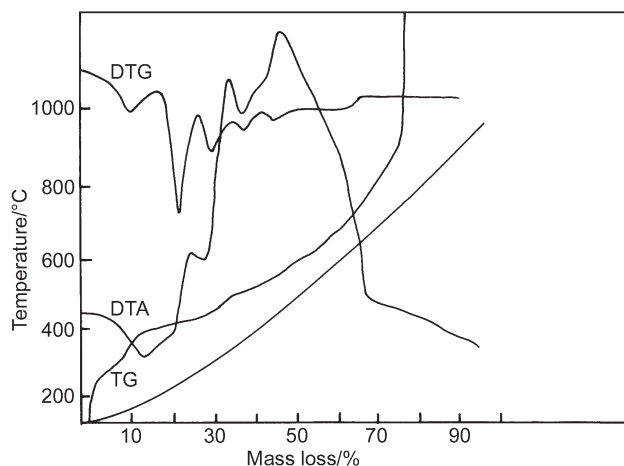


**Fig. 2** Thermal trace of FeC<sub>12</sub>H<sub>22</sub>O<sub>14</sub>·2H<sub>2</sub>O under dynamic nitrogen atmosphere

The d.c. electrical conductivity results for the sample FeC<sub>12</sub>H<sub>22</sub>O<sub>14</sub>·2H<sub>2</sub>O are shown in Fig. 3, by a plot of  $\log \sigma$  vs.  $1/T$ , where  $\sigma$  is the electrical conductivity (ohm cm<sup>-1</sup>) and  $T$  is the temperature in absolute scale. The  $\sigma$  value shows a peak in the region from ambient temperature to 180°C. This peak can be understood as dehydration step [16]. Figure 4(a) shows the X-ray diffraction pattern for ferrous gluconate dihydrate and Fig. 4(b) shows the X-ray diffraction pattern for dehydrated ferrous gluconate. It is seen from these two traces that the crystalline form is lost when dehydration takes place. The infrared spectrum of the sample isothermally heated at 160°C, did not show any bands corresponding to  $\nu_{OH}$ . Elemental analysis also agreed with the composition of the anhydrous formulae, FeC<sub>12</sub>H<sub>22</sub>O<sub>14</sub>. This anhydrous sample was found to be amorphous in nature with X-ray study. The transition from crystalline to amorphous gluconate would possibly indicate the formation of better  $\gamma$ -Fe<sub>2</sub>O<sub>3</sub>, having nanosized particles with high density when carried out under controlled conditions. This transition from amorphous to crystalline phase

results in better properties for ferrites that are prepared by sol-gel techniques [19]. Hence  $\gamma$ -Fe<sub>2</sub>O<sub>3</sub> formed from the thermal decomposition of ferrous gluconate may have better thermal and structural properties when compared to those prepared from thermal decomposition of carboxylates studied earlier by us [16–18]. This is also evident from the saturation magnetisation and coercive force measurements, which are discussed later.

In Fig. 2, after the dehydration peaks the DTA trace shows exothermic peaks at 210, 320, 395 (shoulder) and 440°C. The peaks on the DTG trace were observed at 275, 360, and 415°C. The TG trace shows a two-step mass loss. The first step of mass loss occurred between 160 and 220°C corresponding to the formation of a mixture of FeO and anhydrous gluconate. The electrical conductivity plot shows the presence of a peak in the temperature region 180 to 225°C. A sample isothermally heated in this region (200°C, for 2 h) indicated the presence of FeO in the X-ray diffractogram (Table 1). The infrared spectrum shows a broad band at 550 cm<sup>-1</sup>, which is assigned to Fe–O stretching frequency [16]. In the electrical conductivity trace (Fig. 3) a steady increase in  $\sigma$ -value is noticed with a shoulder around 280°C, later a steep increase in  $\sigma$ -value is noticed upto 460°C thereafter the conductivity trace remained almost constant, which is a typical behaviour for the Fe<sub>3</sub>O<sub>4</sub> [16]. On further heating the final conversion to  $\alpha$ -Fe<sub>2</sub>O<sub>3</sub> takes place. The X-ray diffraction of the sample isothermally heated at 280°C, shows a mixture of FeO and Fe<sub>3</sub>O<sub>4</sub>. The X-ray pattern of the sample isothermally heated at 500°C (2 h), shows the sample to be Fe<sub>3</sub>O<sub>4</sub> (Table 2).

**Table 1** Comparison of X-ray diffraction data of FeO obtained from FeC<sub>12</sub>H<sub>22</sub>O<sub>14</sub>·2H<sub>2</sub>O by heating under dynamic nitrogen at 200°C (2 h)

Observed <i>d</i> -spacing values (μm), present study	Reported [23] <i>d</i> -spacing values μm
4676(40)	
3180(25)	
2889(22)	
2493(75)	2490(80)
2304(20)	
2154(100)	2153(100)
2089(25)	
2058(45)	
1612(10)	
1605(22)	
1524(40)	1523(60)
1300(22)	1299(25)
1134(10)	
1075(9)	1077(15)

Figures in parenthesis show the relative line intensities normalised to the strongest intensity line (given by 100)

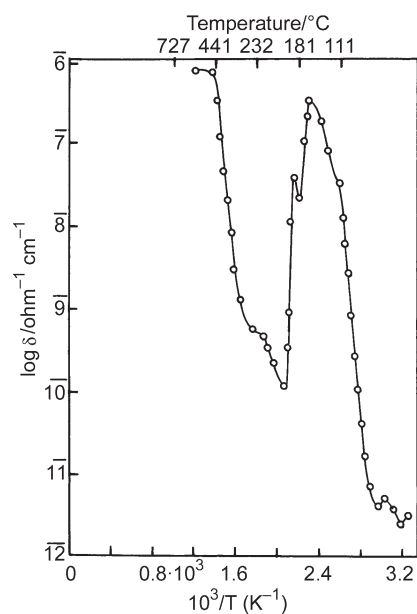


**Fig. 3** d.c. electrical conductivity trace for FeC<sub>12</sub>H<sub>22</sub>O<sub>14</sub>·2H<sub>2</sub>O under nitrogen atmosphere

**Table 2** X-ray data of Fe<sub>3</sub>O<sub>4</sub>, obtained from FeC<sub>12</sub>H<sub>22</sub>O<sub>14</sub>·2H<sub>2</sub>O, by heating under nitrogen atmosphere at 500°C (2 h)

Observed <i>d</i> -spacing values (μm), present study	Fe <sub>3</sub> O <sub>4</sub> , <i>d</i> -spacing in μm [24]
4820(5)	4850(8)
2980(25)	2967(30)
2535(100)	2532(100)
2420(5)	2424(8)
2092(20)	2099(20)
1716(5)	1715(10)
1620(25)	1616(30)
1482(35)	1485(40)
1312(5)	1419(2)
1288(9)	1328(4)
1220(9)	1281(10)
1098(4)	1266(4)
1060(3)	1212(2)
	1122(4)
	1093(12)
	1050(6)

Figures in parenthesis show the relative intensities normalised to that of the strongest line (given by 100)

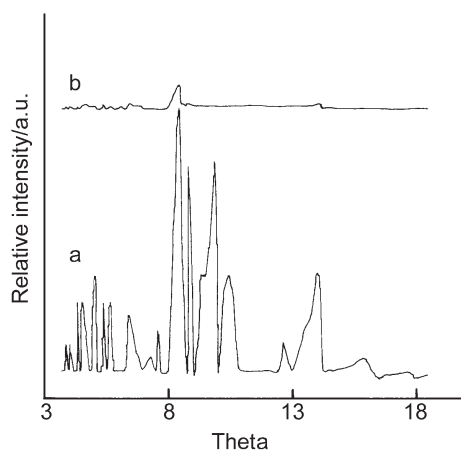


**Fig. 4** XRD pattern for a –  $\text{FeC}_{12}\text{H}_{22}\text{O}_{14} \cdot 2\text{H}_2\text{O}$ ; b – dehydrated  $\text{FeC}_{12}\text{H}_{22}\text{O}_{14} \cdot 2\text{H}_2\text{O}$

#### *Study under dynamic air atmosphere*

The thermal analysis trace for  $\text{FeC}_{12}\text{H}_{22}\text{O}_{14} \cdot 2\text{H}_2\text{O}$  is shown in Fig. 5. The TG trace shows a two-step mass loss. The first step of mass loss occurred in the range from ambient temperature to 160°C, corresponding to partial dehydration of the gluconate. The DTA and DTG traces show peaks at 160 and 178°C. The complete dehydration of the gluconate complex occurs around 230°C, which is noticed on the TG trace, and by an endothermic peak on DTA trace at 220°C.

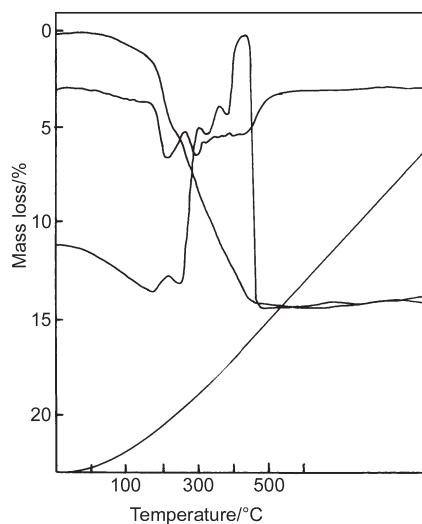


**Fig. 5** Thermal trace of  $\text{FeC}_{12}\text{H}_{22}\text{O}_{14} \cdot 2\text{H}_2\text{O}$  under dynamic air atmosphere

The oxidative decomposition of the complex was indicated by the presence of three exothermic peaks on the DTA trace at 282, 336 and 402°C respectively. The DTG trace also shows peaks at 178 and 265°C. The TG trace shows a continuous mass loss upto 460°C, where a final formation to  $\alpha$ -Fe<sub>2</sub>O<sub>3</sub>, took place. The isothermal heat treatments were given at 290, 340, and 410°C respectively. The X-ray diffraction shows that the sample obtained on isothermal heating at 290°C was a mixture of FeO with some gluconate complex (presence of broad peaks, showing conversion from amorphous to crystalline nature were observed), at 340°C it was a mixture of Fe<sub>3</sub>O<sub>4</sub> and  $\gamma$ -Fe<sub>2</sub>O<sub>3</sub>, and at 410°C the formation of  $\alpha$ -Fe<sub>2</sub>O<sub>3</sub> was complete. Though the amorphous  $\rightarrow$  crystalline transition took place in this atmosphere, from the anhydrous gluconate to formation of different iron oxides, including  $\gamma$ -Fe<sub>2</sub>O<sub>3</sub>, it is observed that the stabilisation of this  $\gamma$ -Fe<sub>2</sub>O<sub>3</sub> was not completely possible on isothermal heating. It is reported in our earlier studies [18] that moisture plays an important role in formation and stabilisation of  $\gamma$ -Fe<sub>2</sub>O<sub>3</sub>, phase formed so. The mechanism for the stabilisation of  $\gamma$ -Fe<sub>2</sub>O<sub>3</sub> phase is understood with the formation of hydrogen ferrite phase with the possible reaction of  $\gamma$ -Fe<sub>2</sub>O<sub>3</sub> and water vapour [12, 18]. The role of water vapour and its subsequent decomposition with the formation of hydrogen ferrite is very important in understanding the doping features of  $\gamma$ -Fe<sub>2</sub>O<sub>3</sub> [12]. Hence, we have carried out our experiments under the influence of dry air containing water vapour to investigate the feasibility of formation of  $\gamma$ -Fe<sub>2</sub>O<sub>3</sub> and its subsequent stabilisation.

#### *Study under dynamic air containing water vapour*

A complete study of direct current electrical conductivity under the atmosphere of dynamic air containing water vapour could not be carried out as the ferrous gluconate pellet melted on heating. The formation of pure  $\gamma$ -Fe<sub>2</sub>O<sub>3</sub> and its stabilisation was possible by isothermally heating the gluconate sample at 360°C for an h in a rotating

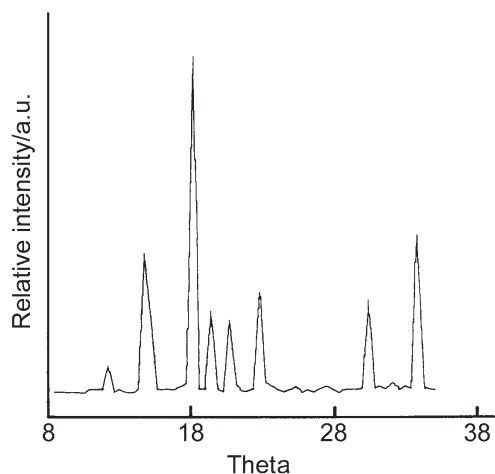


**Fig. 6** XRD pattern of  $\gamma$ -Fe<sub>2</sub>O<sub>3</sub> synthesised by thermal decomposition of FeC<sub>12</sub>H<sub>22</sub>O<sub>14</sub>·2H<sub>2</sub>O under dynamic air containing water vapour atmosphere

### Particle morphology

[illegible]

### Magnetic properties

*J. Therm. Anal. Cal.*, 68, 2002

**Table 3** Magnetic hysteresis results for  $\gamma$ -Fe<sub>2</sub>O<sub>3</sub>

Magnetic property	$\gamma$ -Fe <sub>2</sub> O <sub>3</sub> , obtained in the present study	$\gamma$ -Fe <sub>2</sub> O <sub>3</sub> results from literature [4]
Coercive force/Oe	200	250
Saturation magnetisation/emu g <sup>-1</sup>	59	60
Remanance ratio	0.5	0.6

## Conclusions

- $\gamma$ -Fe<sub>2</sub>O<sub>3</sub> as nanomaterial with required magnetic properties, from the ferrous gluconate precursor, under the atmosphere containing water vapour is obtained.
- It was observed that the water vapour atmosphere stabilises the formation of  $\gamma$ -Fe<sub>2</sub>O<sub>3</sub>, which is in concurrence with earlier studies.
- Under all the atmospheres it was observed that the anhydrous gluconate formed by dehydration of ferrous gluconate dihydrate is amorphous, i.e., a change from crystalline to amorphous phase. This anhydrous ferrous gluconate later converts to crystalline iron oxide. The  $\gamma$ -Fe<sub>2</sub>O<sub>3</sub> obtained from this process, has a cubic structure as revealed from X-ray data.
- $\gamma$ -Fe<sub>2</sub>O<sub>3</sub> obtained in the present study may find application for magnetic recording, heterogeneous catalyst, sensor and for other technological applications.

## References

- 1 D. J. Craik, 'Magnetic Oxides', Vol. 2, Wiley – Interscience, New York 1975.
- 2 D. Bloor, R. J. Brook, M. C. Flemings and S. Mahajan, 'The encyclopaedia of Advanced Materials', Pergamon Press, New York 1993.
- 3 H. Yokoyama et al., Panel displays: High density magnetic recording (ways to 50 nm/bit recording technology), Ferrites: Proceedings of the sixth international conference on ferrites (ICF-6), Tokyo and Kyoto, Japan 1992, p. 1381.
- 4 'Magnetic Recording Hand Book – Technology and Applications', (eds.) C. Denis Mee and Eric D. Daneil, Mc Graw-Hill Co., 1990.
- 5 A. J. Gellman, Current opinion in colloid and interface science, 3 (1998) 368.
- 6 K. Suresh, N. R. S. Kumar K. C. Patil, Adv. Mater. Comm., 30 (1991) 148.
- 7 C. N. R. Rao, J. Mater. Chem., 9 (1999) 1.
- 8 X. Ye, D. Liu, Z. Jio and L. Zhang, J. Phys. D. Application Phys., 31 (1998) 2739.
- 9 G. Monros, J. Carda, M. A. Tena, P. Escibano, J. Badenes and E. Cordoncillo, J. Mater. Chem., 5 (1995) 85.
- 10 H. Sesigur, E. Acma, O. Addemir and A. Tekin, Mater. Res. Bull., 31 (1996) 1573.
- 11 M. C. Blesa, E. Moran, J. D. Tornero, N. Menendaz, E. M. Zamora and J. M. Saniger, J. Mater. Chem., 9 (1999) 227.
- 12 G. S. Chopra, C. Real, M. D. Alcala, L. A. Perez-Maqueda, J. Subrt and J. M. Criado, Chem. Mater., 11 (1999) 1128.
- 13 V. Chhabra, M. Lal, A.N. Maitra and B. Ayyub, Colloid and polymer science, 273 (1995) 939.

- 14 A. Venkataraman, Bull. Mater. Sci., 16 (1993) 51.
- 15 A. Venkataraman and A. J. Mukhedkar, J. Thermal Anal., 36 (1990) 495.
- 16 M. M. Rahaman and A. Venkataraman, Ind. Products Finder (India), 22 (8) (1994) 249.
- 17 A. Venkataraman, M. M. Rahaman, A. K. Nikumbh, V. A. Mukhedkar and A. J. Mukhedkar, Thermochem. Acta, 112 (1987) 237.
- 18 A. Venkataraman, J. Thermal Anal., 46 (1996) 219.
- 19 F. R. Sale and Yt. Chen, Ceram. Trans., 47 (1995) 155.
- 20 ASTM file Number 24–81.
- 21 E. Yihua and Ch. Li, Mater. Chem. and Phys., 51 (1997) 169.
- 22 J. B. Frank, G. Collin, H. Orn and J. McManus, J. Mater. Chem., 9 (1999) 223.
- 23 ASTM file Number 6–615.
- 24 ASTM file Number 19–629.